AJNR

Magnetic resonance imaging of intracranial tumors in children and adolescents.

S B Peterman, R E Steiner and G M Bydder

AJNR Am J Neuroradiol 1984, 5 (6) 703-709
http://www.ajnr.org/content/5/6/703

Magnetic Resonance Imaging of Intracranial Tumors in Children and Adolescents

S. B. Peterman[1]
R. E. Steiner
G. M. Bydder

Magnetic resonance (MR) scans were reviewed of 25 children and adolescents from the age of 9 months to 18 years referred with a suspected or proven diagnosis of intracranial tumor. Twenty-one of these children had MR scans positive for tumor. Histology was available in 14. The other seven patients were managed clinically as cases of cerebral tumor, although histologic confirmation was lacking. Seventeen tumors displayed an increase in both T1 and T2. One dermoid tumor and part of another displayed a very short T1 (less than that of white matter). Two hamartomas had T1s similar to that of gray matter and a small increase in T2. Four of the children did not show MR or computed tomographic (CT) evidence of intracranial tumors. Follow-up of these cases for 1–23 months after the MR and CT studies revealed no subsequent clinical evidence of tumor. MR scans showed more extensive abnormality than did third-generation CT scans in eight of 10 cases and more extensive abnormality than EMI CT 1010 scans in 10 of 11 cases. Mass effects were better demonstrated in 14 of the 16 patients in whom they were seen. CT demonstrated calcification better than did MR in all four cases in which it was identified. The tumor-edema interface was shown better on CT in each of the three cases with contrast enhancement on CT. MR is a sensitive method of evaluating intracranial tumors in children and adolescents.

Magnetic resonance imaging (MRI) is a sensitive method for evaluating tumors in adults [1–3]; however, few intracranial tumors have been described in children [4, 5]. Adult cerebral tumors are recognized as a result of their increased T1 and T2, mass effects, edema, and loss of contrast between gray and white matter. MRI is especially useful in detecting posterior fossa tumors because of its lack of bone artifact [6–8]. MRI in children differs from that in adults. The normal brain of infants has a long T1 and T2 because of its greater water content and lower level of myelination [9, 10]. Children also display a spectrum of intracranial tumors different from that of adults. Many tumors are located in the posterior fossa, where they are advantageously demonstrated with MRI. The lack of hazard associated with MRI [11, 12] is a factor of significant importance in evaluating children. The National Radiological Protection Board (NRPB) reports that no unacceptable effects have been observed in isolated tissues, intact animals, or humans when the MR examination has been performed within its guidelines [13]. We reviewed our experience with MR in imaging intracranial tumors in children and adolescents.

Received February 8, 1984; accepted after revision June 13, 1984.

[1] All authors: Department of Diagnostic Radiology, Royal Postgraduate Medical School, Hammersmith Hospital, Du Cane Rd., London W12 0HS, United Kingdom. Address reprint requests to R. E. Steiner.

AJNR 5:703–709, November/December 1984
0195–6108/84/0506–0703

Materials and Methods

Records and MR scans were reviewed of all 104 children and adolescents (32 weeks postmenstrual age to 18 years) examined in the Hammersmith Hospital MR unit during the years 1981–1983. At the time of referral, 23 had clinically suspected intracranial tumor, and two had clinically suspected recurrence of histologically confirmed intracranial tumor.

The MR scans were positive for tumor in the two patients with histologically confirmed intracranial tumor and in 19 of those with clinically suspected intracranial tumor. Subsequent histologic confirmation was available in another 12 of these cases (total of 14 cases). The

TABLE 1: **Distribution of Pediatric Intracranial Tumors**

Type	No.
Tumors with histologic proof:	
Tumors of neuroepithelial tissue:	
Astrocytoma:	
Grade I	2
Low-grade	1
Grade III	1
Malignant glioma	1
Glioblastoma multiforme	1
Tumors of meningeal and related tissues:	
Fibrosarcoma (poorly differentiated)	1
Primary malignant lymphomas:	
Microglioma	1
Malformative tumors and tumorlike lesions:	
Craniopharyngioma	1
Dermoid cyst	2
Hamartoma	2
Vascular malformations:	
Cavernous angioma	1
Tumors without histologic proof:	
Infratentorial tumors	5
Supratentorial tumor	1
Acute lymphocytic leukemia	1

other seven patients had no histologic proof of tumor but received treatment after clinical and MR diagnosis of tumor. The final diagnoses of the 21 cases are listed in table 1, using the WHO classification of intracranial tumors [14].

Four patients with clinically suspected intracranial tumors did not display MR findings of tumor. One had an MR diagnosis of brainstem encephalitis and subsequently improved without specific treatment. The second had hydrocephalus without computed tomographic (CT) or MR evidence of a tumor and was presumed to have an aqueduct stenosis after meningitis. The other two cases had intracranial calcification on CT without evidence of associated tumor on CT or MR. Follow-up of these four cases from 1 to 23 months showed no subsequent clinical evidence of intracranial tumor.

All MR examinations were done with the approval of the Research Ethics Committee of the Royal Postgraduate Medical School following guidelines proposed by the NRPB [13]. Informed consent was obtained from each parent or guardian before scanning. Oral chloral hydrate (50–100 mg/kg) or oral trimeprazine (6–8 mg/kg) was given for sedation 30–60 min before the examination of infants or children up to the age of 4 years. A surface respiratory monitor was placed on the sedated children.

The MR scanner used in this study was described previously [15]. It is based on a superconducting magnet with a static magnetic field of 0.15 T. Radiofrequency pulses at 6.5 MHz are used to perturb protons, following which an electrical signal is detected by a receiver coil surrounding the patient's head. Magnetic field gradients are used to spatially encode the electrical signal. Image reconstruction is performed by Fourier transform followed by projection reconstruction or by two-dimensional Fourier transform.

Saturation-recovery (SR), inversion-recovery (IR), and spin-echo (SE) pulse sequences were employed. An inversion time (T1) of 600 msec was used in the IR sequence on children up to 4 years of age, and one of 400 msec was used on the older children. The different pulse sequences produced images with varying dependence on proton density (ρ), T1, and T2 as previously described [4, 7].

All 21 children had CT scans (19 with contrast enhancement). These were obtained on an EMI CT 1010 (11 cases), a Siemens Somatom II (seven cases), a Philips Tomoscan 310 (two cases), or a GE CT/T 8800 (one case) scanner. Three children also had CT studies with metrizamide. Two children had myodil cisternography, 10 had angiography (four carotid studies, five vertebral studies, one carotid and vertebral study), and one had a myodil ventriculogram.

Fig. 1.—Low-grade astrocytoma. Sagittal IR 1400/400 (**A**) and SE 1080/80 (**B**) scans. Area of long T1 extends from pons to C6 (**A**). Cervical cord is widened with higher signal intensity from pons to C2 (site of previous radiotherapy) than from C2 to C6 (site of presumed tumor recurrence).

Results

No short-term side effects of the MR examinations were noted. Movement of the child resulted in streak artifacts at the margins of the images. Ventricular shunts produced local artifacts on the images when included in the imaging plane. A central artifact of a black and white dot was seen in many of the projection reconstruction images.

Tumors with Histologic Proof: Neuroepithelial Tissue

Astrocytoma. Astrocytomas were demonstrated in four children. One tumor was supratentorial, two were in the cerebellum, and one was in the brainstem. MRI demonstrated cystic structures in two lesions, of which one lesion was shown to have a cyst on CT. Two of the astrocytomas had areas of low signal intensity on the SE 1080/80 sequence that corresponded to calcification better demonstrated on CT.

One tumor had been demonstrated in the brainstem and upper cervical cord with CT 3 years before the MR scan and had been treated with radiotherapy. The MR scan, obtained because of clinical evidence of recurrence, displayed an expanded brainstem and cervical cord from the lower pons to C6 (fig. 1). The SE 1080/80 signal intensity was lower at the site of presumed recurrence (C2–C6) then at the site of previous radiotherapy (pons to C6). After MRI, additional radiation therapy was applied to the C2–C6 region with clinical improvement.

Malignant glioma. A 15-year-old boy was referred with a CT scan displaying a patchy, low-attenuation region with an associated mass effect in the left frontal lobe. More extensive changes were seen with MR (fig. 2). Craniotomy confirmed the diagnosis of intracerebral tumor, and histology showed a malignant glioma.

Glioblastoma multiforme. A 12-year-old boy had a negative

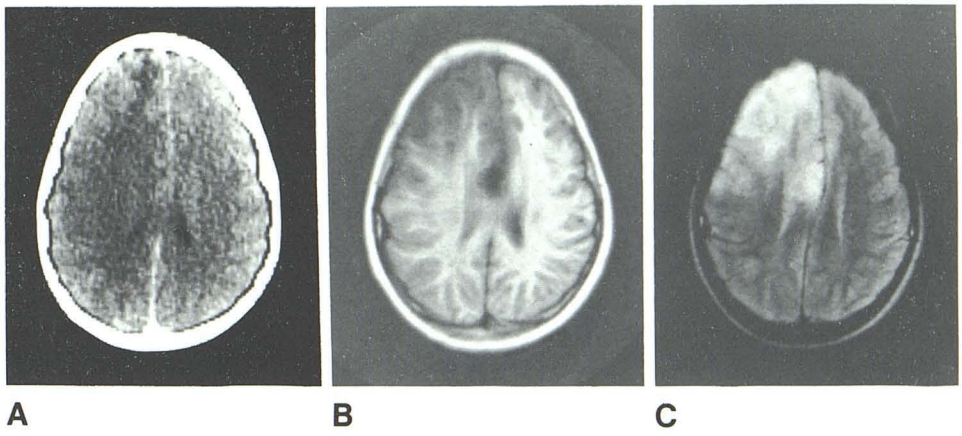

Fig. 2.—Malignant glioma. Contrast-enhanced CT (**A**), IR 1500/500/44 (**B**), and SE 1580/80 (**C**) images. Poorly defined low-attenuation region in left frontal lobe with associated mass effect (**A**). More extensive abnormality is seen with long T1 and T2 (**B** and **C**).

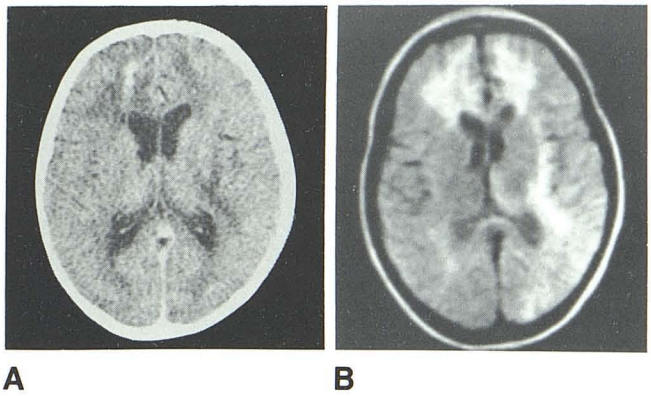

Fig. 3.—Microglioma. Contrast-enhanced CT (**A**) and SE 1080/80 (**B**) scans. Contrast-enhancing lesion in left frontal lobe is surrounded by area of low attenuation; low-attenuation areas are seen also in right frontal and basal ganglia regions (**A**). Areas of increased T2 are seen in both frontal lobes, right basal ganglia, and both temporoparietal regions as well (**B**).

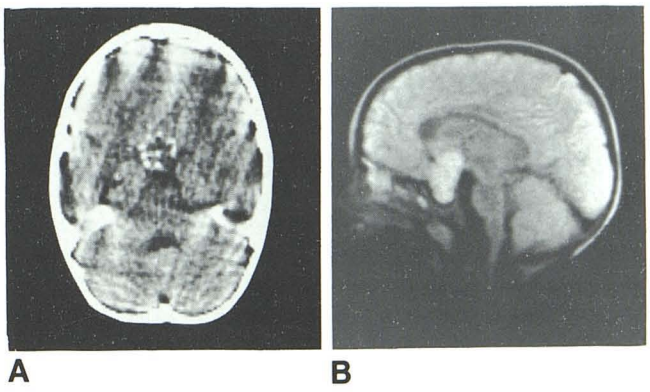

Fig. 4.—Craniopharyngioma. CT (**A**) and sagittal SE 1580/80 (**B**) images. Calcification in sellar and parasellar regions (**A**). Tumor has slightly increased T2 and extends through sella into sphenoid sinus (**B**).

EMI CT 1010 scan followed by a Siemens Somatom II scan that showed rotation of the fourth ventricle. Extensive changes were seen with MR in the left pons and cerebellar hemisphere. The patient was treated with radiotherapy but died 7 months later. The pathologic diagnosis was glioblastoma multiforme. Close correspondence was seen between the MR scan and the postmortem changes.

Tumors with Histologic Proof: Meningeal and Related Tissues

Fibrosarcoma. An extensive intraaxial tumor was demonstrated with MR in an 8-year-old girl. The internal structure of the lesion was seen on both IR and SE sequences. The tumor was subsequently excised, and histology showed poorly differentiated fibrosarcoma.

Tumors with Histologic Proof: Primary Malignant Lymphomas

Microglioma. An 8-year-old boy had a history of episodic headache and personality changes that resolved with steroid therapy. CT scans during symptomatic periods displayed mutliple enhancing lesions surrounded by areas of low attenuation in both frontal lobes and the right temporoparietal lobe without mass effects. These resolved on CT during asymptomatic periods. Extensive loss of gray-white matter contrast with areas of long T1 and T2 were seen in both hemispheres on an MR scan when the patient was symptomatic (fig. 3). An MR scan was not obtained when the patient was asymptomatic. Stereotactic biopsy gave the histologic diagnosis of microglioma.

Tumors with Histologic Proof: Malformative Tumors and Tumorlike Lesions

Craniopharyngioma. A 4-year-old boy had calcifications in the sellar and parasellar region on CT. MRI demonstrated a lesion with a slightly increased T2 extending through the sella into the sphenoid sinus (fig. 4). The calcification was not detected with MRI. The diagnosis of craniopharyngioma was confirmed at surgery.

Dermoid cyst. Two children with dermoid cysts were scanned. A 12-year-old girl had an isodense parasellar lesion on CT. The sagittal MRI view demonstrated the craniocaudal

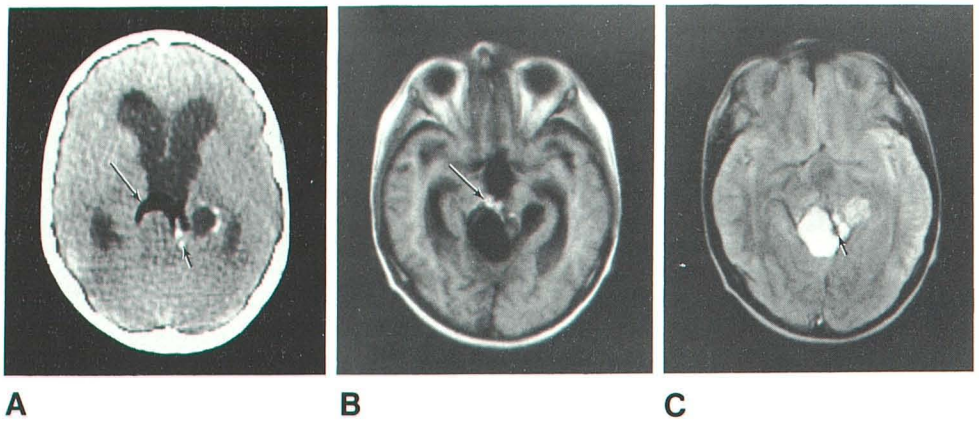

Fig. 5.—Dermoid cyst after partial resection and radiotherapy. Contrast-enhanced CT (**A**), IR 1500/500/44 (**B**), and SE 1580/80 (**C**) images. **A**, Area of low attenuation (*long arrow*) and calcification (*short arrow*) is seen in region of pineal gland. **B** and **C**, Short T1 component of tumor (*long arrow*) is anterior to area of long T1 and T2, consistent with cyst. **A** and **C**, Calcification has low signal intensity on MRI (*short arrows*). Moderate hydrocephalus is present on all scans. (CT scan [**A**] is more steeply angulated than MR scans [**B** and **C**].)

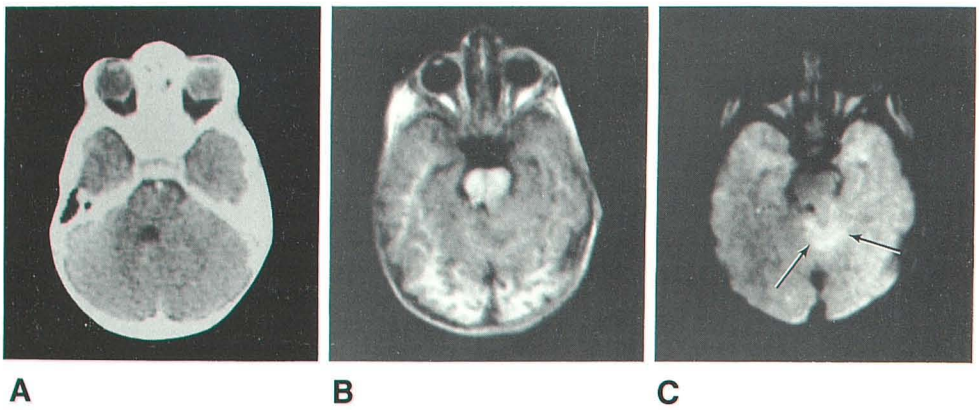

Fig. 6.—Hamartoma. Contrast-enhanced CT (**A**), IR 1800/600 (**B**), and SE 1580/80 (**C**) scans. Displacement of fourth ventricle to left is seen on CT (**A**). Lesion with T1 similar to that of gray matter and increased T2 (*arrows*) is demonstrated on MRI (**B** and **C**).

extent of the tumor with inferior extension into the sphenoid sinus. The tumor had a very short T1 and a slightly increased T2. Surgery gave the histologic diagnosis of a dermoid cyst.

A 17-year-old boy had partial resection of a dermoid cyst in the region of the pineal gland 2 years previously and had undergone radiation therapy. Since then CT scans had shown calcification and areas of low attenuation in the region of the tumor with a moderate degree of hydrocephalus. On MRI the tumor, which had a short T1 and a slightly increased T2, was next to an area of long T1 and T2, consistent with a cyst (fig. 5). Areas of low proton density corresponded to the calcification on CT.

Hamartoma. Two children had hamartomas. The first, a 9-month-old girl with precocious puberty, had a hamartoma of the thalamus and prepontine region. The second, a 16-month-old boy, had a cerebellar hamartoma. On CT both lesions were isodense and nonenhancing with mass effect. On MRI the tumors had a T1 similar to that of gray matter and a slightly increased T2 (fig. 6). Excision of the tumors gave the histologic diagnosis.

Tumors with Histologic Proof: Vascular Malformations

Cavernous angioma. A CT scan on a 13-year-old boy demonstrated a nonenhancing brainstem lesion containing hematoma. The MR scan showed areas of long T1 and T2 in an expanded mesencephalon (fig. 7). An area of short T1 on the transverse scan and several areas of long T2 on the sagittal scan corresponded to the region of hematoma on CT. Surgery revealed several solid and liquid hematomas posteriorly. There was a calcified mass slightly deeper to the hematomas surrounded by small, thin-walled blood vessels. This was believed to be a cavernous angioma.

Tumors without Histologic Proof: Infratentorial

Five patients had MRI evidence of infratentorial intraaxial tumors without histologic confirmation. Four underwent radiation therapy on the basis of their clinical and MR examinations, and all improved clinically. CT showed low-attenuation brainstem lesions in each of the four patients with displacement of the fourth ventricle in two cases. MRI demonstrated the tumors as areas of nonuniformly increased T1 and T2 (fig. 8). One child had an area of very long T1 that matched an area of low attenuation on CT. This was consistent with either a cyst within the tumor or a dilated fourth ventricle. Post-radiation-therapy scans were obtained 2, 4, and 7 months after therapy in another child. The tumor size was reduced on the second scan, remained stable on the third scan, and had increased on the fourth scan. The child had been improved clinically until the last scan, when her condition had worsened.

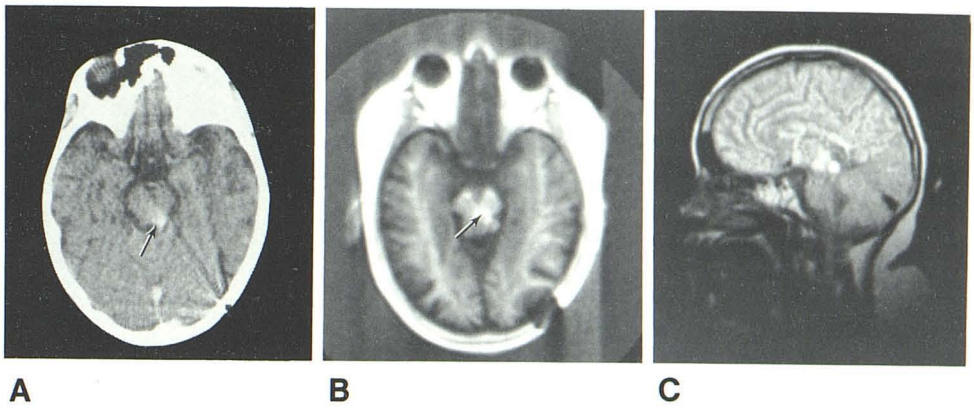

Fig. 7.—Cavernous angioma. Contrast-enhanced CT (**A**), IR 1400/400 (**B**), and sagittal SE 1080/80 (**C**) scans. Area of hemorrhage in region of right inferior colliculus on CT (**A**) corresponds to area of short T1 on MRI (**B**) (*arrows*). Region of long T1 is seen in posterior mesencephalon. Three distinct, circular lesions of long T2 are in expanded mesencephalon (**C**). Artifact in right parietal region is secondary to ventricular shunt (**A** and **B**).

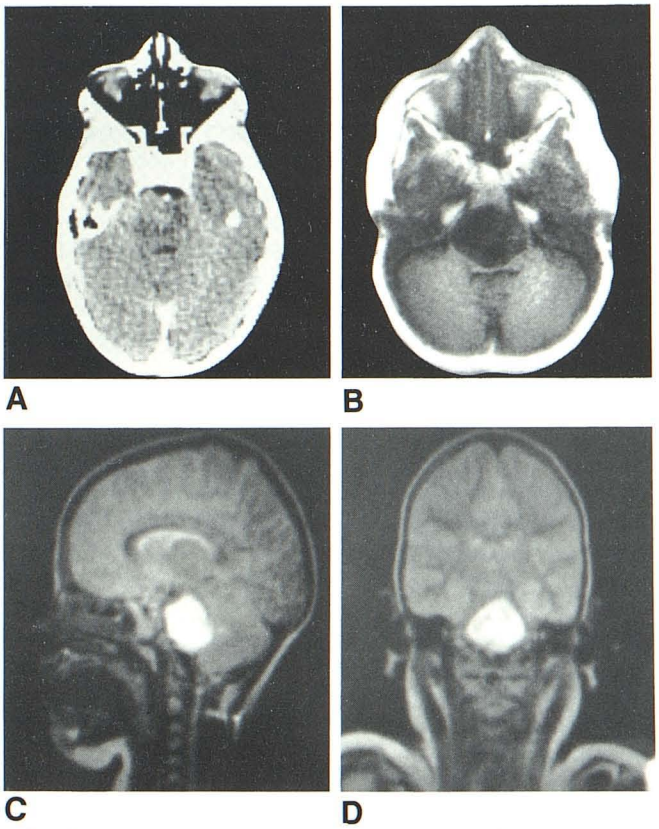

Fig. 8.—Infratenorial, intraaxial tumor without histology. Contrast-enhanced CT (**A**), IR 1400/400/44 (**B**), sagittal SE 1160/160 (**C**), and coronal SE 1160/160 (**D**) images. Low-attenuation lesion in pons (**A**). Brainstem is expanded with long T1 and T2 (**B–D**).

The fifth patient had an expanded medulla on metrizamide-enhanced CT. MRI showed a widened medulla and upper cervical cord without a change in T1 or T2. She was treated conservatively.

Tumors without Histologic Proof: Supratentorial

One child had a temporal lobe lesion on CT and MR. This was clinically thought to be benign and was not biopsied.

Tumors without Histologic Proof: Acute Lymphocytic Leukemia

A 16-year-old boy with acute lymphocytic leukemia of the central nervous system was treated with radiation therapy and intrathecal methotrexate 8 years before MRI. Areas of long T1 and T2 were seen in the right frontal and parietal lobes with separate areas of increased T2 periventricularly. It was unclear whether these changes were from tumor recurrence, edema, radiation therapy, or chemotherapy. The patient died 5 months later, but no postmortem was performed.

Comparison with CT

Ten of the children and adolescents had had CT scans on third-generation CT scanners (Siemens Somatom II, Philips Tomoscan 310, or GE CT/T 8800). MRI showed more extensive abnormality than did CT in eight of these patients and a similar extent in two. Mass effects were better demonstrated with MRI in all seven cases in which they were seen. MRI showed cysts or necrosis in the tumors of four patients, of which two had no internal structure demonstrated on CT. Hemorrhage was shown distinctly on both CT and MRI in one patient and only on CT in another (both types of scans were obtained on the same day). In one patient, calcification was seen on CT and was suspected on MRI as an area of low signal intensity. The calcification appeared more extensive on CT. Two tumors enhanced on contrast-enhanced CT. The tumor-edema interface was better demonstrated with CT in both patients.

Eleven of the patients had had CT scans with an EMI CT 1010 scanner. This is an older model of CT scanner and therefore not well suited for detailed comparison with MRI. MRI showed more extensive abnormality than CT in 10 of these patients and a similar extent in one. Mass effects were better demonstrated on MRI in seven of the nine patients in which they were seen. They were seen equally well on both MRI and CT in the other two patients. MRI showed cysts or necrosis in the tumors of three patients that were not seen on CT. Hemorrhage was distinctly shown on both CT and MRI in one patient. It was seen only on MRI in another; however, the MR scan was obtained 10 days after the CT scan. Calcification was demonstrated on CT and suspected

on MRI as areas of low signal intensity in two patients. It appeared more extensive on CT in both cases. In the patient with a craniopharyngioma, calcification was seen on CT and was not suspected on MRI. The tumor-edema interface was better seen on CT in the one patient with a contrast-enhancing lesion on CT.

Discussion

Intracranial tumors in children and adolescents usually have the nonspecific MRI finding of an increased T1 and T2. The dermoid tumors were notable for a very short T1 (less than that of white matter), which was probably because of the high lipid content of the sebaceous material within the tumors. The malformative tumors (two hamartomas and one craniopharyngioma) had a T1 similar to that of gray matter and a slightly increased T2.

The internal structure of the tumors is well demonstrated on MR scans. Cysts have a longer T1 and T2 than do solid tumors. Areas of necrosis also have a long T1 and T2. Hemorrhage and hematoma have a short T1 and long T2. Calcification has a low proton density. Thus, it has a very low signal intensity, and its presence can only be suspected on MRI. Vascular tumors with high blood flow may be marked by bright areas on the SR scan [16]. These bright areas were not present in the patient with the cavernous angioma; however, the tumor had evidence of previous thrombosis.

Peritumoral edema has a long T1 and T2. Benign tumors generally have less peritumoral edema than do malignant tumors. On MRI it is difficult to define the tumor-edema interface. Edema tends to be confined in white matter, whereas tumor crosses gray-white matter boundaries. Paramagnetic contrast agents, which shorten T1 and T2, have proved successful in defining this interface in adults [17] and may be important in children as well.

The gray/white-matter interfaces seen on IR scans provide an additional marker of mass effects. These interfaces are better seen in older children, since there is little myelination in infants. MRI demonstrates hydrocephalus, and periventricular areas of long T2 imply that the hydrocephalus is acute or subacute.

Eleven of the 21 patients had CT scans with an EMI CT 1010 scanner, and thus a detailed comparison between CT and MRI in this series would be biased in favor of MRI. However, several general observations can be made about the two methods of examination: Calcification is an important sign in the assessment of tumors. On CT, the presence and extent of calcification is well demonstrated. However, on MRI, its presence can only be suspected. Contrast-enhanced CT scans define the tumor-edema interface better than do nonenhanced MRI scans.

MRI shows more extensive abnormality than does CT. Various types of gliomas can be missed initially on CT [18], and MRI has been reported to demonstrate gliomas that were not seen on CT [1, 19]. Internal structure and extension of the tumor are better demonstrated by MRI. The direct coronal and sagittal slices of MRI are well suited for midline lesions. MRI is particularly effective in diagnosing posterior fossa tumors with the increase in T1 and T2 of the tumor, the lack of bone artifact, and the use of sagittal slices. These tumors are isodense and often nonenhancing on CT [20]. A metrizamide CT scan is usually indicated, which is invasive and shows external expansion rather than the internal extension of the tumor.

Scanning time is shorter with CT than with MRI; however, both require infants and small children to be sedated. The development of volume scanning [21] and multislice scanning [22] has significantly cut the total examination time for MRI. MRI is without hazard, and thus referral can be made at the earliest clinical suspicion of intracranial tumor.

The results of an MR scan are somewhat nonspecific. Most intracranial tumors have a long T1 and T2, although lipid-containing tumors appear to be marked by a very short T1. Thus, the MRI differential diagnosis of a tumor is primarily dependent, as with CT, on the site of the tumor and the age and gender of the patient. The finding of an increased T1 and T2 can be not only from an intracranial tumor but also from other intracranial processes such as infection, inflammation, or demyelinating disease. An increased T1 and T2 on a post-therapeutic scan can be from recurrent tumor, long-term changes secondary to radiation therapy, or postchemotherapy periventricular leukoencephalopathy. As larger numbers of patients are studied and more experience is gained with paramagnetic contrast agents, MRI may become more specific. However, it is already an effective, sensitive, and hazardless method of evaluating intracranial tumors in children and adolescents.

ACKNOWLEDGMENTS

We thank the Department of Health and Social Security, particularly Gordon Higson and John Williams, for support and encouragement.

REFERENCES

1. Buonanno FS, Pykett IL, Brady TJ, et al. Clinical relevance of two different nuclear magnetic resonance (NMR) approaches to imaging of a low grade astrocytoma. *J Comput Assist Tomogr* **1982**;6:529–535
2. Bydder GM, Steiner RE, Young IR, et al. Clinical NMR imaging of the brain: 140 cases. *AJNR* **1982**;3:459–480, *AJR* **1982**; 139:215–236
3. Brant-Zawadzki M, Davis PL, Crooks LE, et al. NMR demonstration of cerebral abnormalities: comparison with CT. *AJNR* **1983**;4:117–124, *AJR* **1983**;140:847–854
4. Johnson MA, Pennock JM, Bydder GM, et al. Clinical NMR imaging of the brain in children: normal and neurologic disease. *AJNR* **1983**;4:1013–1026, *AJR* **1983**;141:1005–1018
5. Zimmerman RA, Bilaniuk LT, Goldberg HI, et al. Cerebral NMR imaging: early results with a 0.12 T resistive system. *AJNR* **1984**;5:1–7, *AJR* **1983**;141:1187–1193
6. Bydder GM, Steiner RE, Thomas DJ, Marshall J, Gilderdale DJ, Young IR. Nuclear magnetic resonance imaging of the posterior fossa: 50 cases. *Clin Radiol* **1983**;34:173–188
7. Randell CP, Collins AG, Young IR, et al. Nuclear magnetic resonance imaging of posterior fossa tumors. *AJNR* **1983**;4:1027–1034, *AJR* **1983**;141:489–496
8. McGinnis BD, Brady TJ, New PFJ, et al. Nuclear magnetic

resonance (NMR) imaging of tumors in the posterior fossa. *J Comput Assist Tomogr* **1983**;7:575–584
9. Smith JF. Central nervous system. In: Berry CL, ed. *Pediatric pathology*. Berlin: Springer-Verlag, **1981**:147–148
10. Yakolev PI, Lecours AR. The myelogenetic cycles of regional maturation in the brain. In: Minkowski A, ed. *Regional development of the brain in early life*. Oxford: Blackwell Scientific, **1967**:3–69
11. Saunders RD. Biological hazards of NMR. In: Witcofski RL, Karstaedt N, Partain CL, eds. *NMR imaging*. Winston-Salem, NC: Bowman Gray School of Medicine, **1981**:65–71
12. Reid A, Smith FW, Hutchinson JMS. Nuclear magnetic resonance imaging and its safety implications: follow-up of 181 patients. *Br J Radiol* **1982**;55:784–786
13. National Radiological Protection Board *ad hoc* Advisory Group on Nuclear Magnetic Resonance Clinical Imaging. Revised guidance on acceptable limits of exposure during nuclear magnetic resonance clinical imaging. *Br J Radiol* **1983**;56:974–977
14. Zulch KJ (in collaboration with pathologists in 14 countries). *Histological typing of tumours of the central nervous system*, WHO international classification of tumours, no. 21. Geneva: World Health Organization: **1979**
15. Young IR, Burl M, Clarke GJ, et al. Magnetic resonance properties of hydrogen: imaging the posterior fossa. *AJNR* **1981**;2:487–493, *AJR* **1981**;137:895–901
16. Young IR, Bydder GM, Hall AS, et al. NMR imaging in the diagnosis and management of intracranial angiomas. *AJNR* **1983**;4:837–838
17. Carr DH, Brown J, Bydder GM, et al. Clinical use of intravenous gadolinium-DTPA as a contrast agent in NMR imaging of cerebral tumours. *Lancet* **1984**;1:484–486
18. Wulff JD, Proffitt PQ, Panszi JG, Ziegler DK. False-negative CT's in astrocytomas: the value of repeat scanning. *Neurology* (NY) **1982**;32:766–769
19. Gräfin von Einsiedel H, Löffler W. Nuclear magnetic resonance imaging of brain tumours unrevealed by CT. *Eur J Radiol* **1982**;2:226–234
20. Bilaniuk LT, Zimmerman RA, Littman P, et al. Computed tomography of brain stem gliomas in children. *Radiology* **1980**;134:89–95
21. Lai C-M, Lauterbur PC. True three-dimensional image reconstruction by nuclear magnetic resonance zeugmatography. *Phys Med Biol* **1981**;26:851–856
22. Crooks LE, Ortendahl DA, Kaufman L, et al. Clinical efficiency of nuclear magnetic resonance imaging. *Radiology* **1983**;146:123–128